Physical origin of dynamical stimulated Brillouin scattering in optical fibers with feedback

Dejin Yu,* Weiping Lu, and Robert G. Harrison
Department of Physics, Heriot-Watt University, Riccarton, Edinburgh EH14 4AS, United Kingdom
(Received 21 April 1994)

The role of spontaneous scattering and nonlinear refraction on the nonlinear dynamics of stimulated Brillouin scattering with feedback is investigated. We find that feedback suppresses stochasticity in the amplification process of the Stokes emission, giving rise to deterministic behavior, the forms of which are found to be critically dependent on the strength of the nonlinear refraction, which is shown to depend on the polarization-preserving properties of the medium. Our results provide an explanation of the chaotic dynamics observed in polarization scrambled fibers and also account for the simpler forms of dynamical behavior reported using polarization-preserving fibers.

PACS number(s): 42.65.Es, 05.45.+b, 41.20.−q, 42.79.−e

Recent experimental investigations of stimulated Brillouin scattering (SBS) in single-mode optical fibers with external feedback have established the Stokes emission to exhibit highly deterministic dynamics from the onset of SBS oscillation [1–5]. Periodic and quasiperiodic behavior is found to be common in fibers with various polarization properties, while in non-polarization-preserving fibers chaos evolving from the quasiperiodicity has also been recently observed [1]. These features contrast with the aperiodic behavior of the Stokes emission observed in fibers without feedback [2,3,6], the stochastic nature of which has been attributed to the role of spontaneous Brillouin scattering, which initiates the SBS process [3,7]. Conversely, for SBS with feedback, spontaneous scattering would seem to have little influence on the temporal structure of the Stokes emission, the dynamics of which nevertheless appears to be critically dependent on the fiber type. In this paper we address theoretically these issues by accounting for spontaneous emission and the role of nonlinear refraction [8,9], in particular, the enhanced effect of the latter arising from the polarization-preserving properties of the medium. Our findings show that over broad operating conditions feedback (even weak) does indeed suppress stochasticity in the amplification process of the Stokes emission, giving rise to deterministic features, the forms of which, whether simple or complex, are found to be critically dependent on the strength of the nonlinear refraction. Our results provide an explanation of the chaotic dynamics observed in polarization-scrambled fibers [1] and also account for the simpler forms of dynamic behavior reported using polarization-preserving fibers [3].

Stimulated Brillouin scattering is described classically as a three-wave parametric coupling process between two electromagnetic waves, the pump and Stokes, and an acoustic wave [10]. In an optical fiber, only the backward scattering is involved because the frequency shift of the Stokes wave vanishes in the forward direction. A generalized description of this interaction accounting for nonlinear refraction was analyzed by Lu and Harrison [8]. With the inclusion of noise initiation and weak feedback, the full model description in normalized form becomes

$$\frac{\partial A}{\partial \eta}+\frac{\partial A}{\partial \xi}+\frac{1}{2}\beta A=-gBC+iu[|A|^2+2|B|^2]A\ , \tag{1}$$

$$\frac{\partial B}{\partial \eta}-\frac{\partial B}{\partial \xi}+\frac{1}{2}\beta B=gAC^*+iu[|B|^2+2|A|^2]B\ , \tag{2}$$

$$\frac{1}{\beta_A}\frac{\partial C}{\partial \eta}+C=AB^*+f(\eta,\xi)\ , \tag{3}$$

$$\frac{\partial D}{\partial \eta}+\frac{\partial D}{\partial \xi}+\frac{1}{2}\beta D=2iu[|A|^2+|B|^2]D\ , \tag{4}$$

where for the case of weak feedback ($R_1R_2\ll 1$) the boundary conditions are simplified to

$$D(\eta,\xi=0)=\sqrt{R_1}B(\eta,\xi=0)\ , \tag{5}$$

$$B(\eta,\xi=1)=\sqrt{R_2}D(\eta,\xi=1)\ , \tag{6}$$

where A,B,C, and D are the slowly varying amplitudes of the forward-going pump, backward-going Stokes fields, the acoustic wave, and the forward-going Stokes field normalized to incident pump amplitude A_0 at $z=0$, respectively. $f(\eta,\xi)$ is the Langevin noise source describing the random thermal fluctuation of the density in order to include the effect of the Gaussian white noise [6,7]. $\eta=t/T_r$ and $\xi=z/L$ are normalized time and space coordinates and $T_r=nL/c$ is the transit time of the light waves in the fiber of the length L. $\beta=\alpha L$ and $\beta_A=\pi\Delta\nu_B T_r$ are the normalized power loss of light waves and the relaxation rate of sound in the medium and α and $\Delta\nu_B$ are the loss coefficient and the spontaneous Brillouin linewidth, respectively.

In obtaining Eqs.(1)–(4), two contributions to nonlinear polarization are considered, namely, electrostriction and intensity-dependent refraction, as in Refs. [8,9]. The former causes the nonlinear gain of the Stokes wave and the latter results in self- and cross-phase modulations due to the presence of the light fields. They are deter-

*FAX: 031-451 3136. Electronic address: PHYDY@UK.AC.HW.VAXA

mined respectively through the control parameters g and u in these equations and depend not only on the material, but also on the polarization-preserving properties of the fiber, whether polarization preserved or scrambled. The gain g is given by

$$g=\frac{P_0 g_0 KL}{2A_{\text{eff}}\delta_e} , \tag{7}$$

where P_0 is the incident pump power, A_{eff} is the effective area of the acousto-optic interaction, and g_0 is the conventional peak Brillouin gain coefficient, which in our analysis is modified to $g_b=g_0K/\delta_e$, where δ_e is the enlargement factor of Brillouin bandwidth in the fiber [11,12]. K is a depolarization factor defined in the literature as $K=\overline{(\mathbf{e}_1\cdot\mathbf{e}_2)^2}$, in which $\mathbf{e}_1$ and $\mathbf{e}_2$ are the local unit vectors of the pump and Stokes waves in the fiber. In this paper we restrict our considerations to the cases of polarization-scrambled and polarization-preserving fibers, for which we show below $K=\frac{1}{2}$ and 1, respectively. In order to understand the dependence of u on the depolarization factor K, we consider the third-order nonlinear polarization component P_x of the two orthogonally polarized components of a single light wave in a fiber. This is given by [10,13]

$$P_x=\frac{3\varepsilon_0}{4}\chi^{(3)}[|E_x|^2+\tfrac{2}{3}|E_y|^2]E_x , \tag{8}$$

where the first term is associated with self-phase modulation and the second one is responsible for cross-phase modulation. For the polarization-scrambled fiber, the polarization direction of an initially linearly polarized field becomes random over a short propagation distance and, as a result, statistically $|E_x|^2=|E_y|^2$ and $E_xE_y^*=0$. For the polarization-preserving fiber, we assume the field to be polarized in the x direction and $E_xE_y^*=0$ is naturally satisfied. Defining a polarization factor κ to describe the proportion of the intensity in the x direction as

$$\kappa=\frac{|E_x|^2}{|E_x|^2+|E_y|^2} , \tag{9}$$

it ranges from $\frac{1}{2}$ to 1, the two limits corresponding to polarization-scrambled and polarization-preserving fiber, respectively. The relation between K and κ is easily obtained according to their definitions to be $K=\kappa^2+(1-\kappa)^2$ for the two cases $K=\frac{1}{2}$ and 1 to be considered below. By substituting Eq. (9) into Eq. (8) we obtain

$$\begin{aligned}P_x&=\frac{3\varepsilon_0}{4}\chi^{(3)}\left[1+\frac{2}{3}\frac{|E_y|^2}{|E_x|^2}\right]|E_x|^2E_x\\&=\frac{3\varepsilon_0}{4}\chi^{(3)}\left[\frac{2+\kappa}{3\kappa}\right]|E_x|^2E_x .\end{aligned} \tag{10}$$

As can be seen Eq. (10) gives an enhancement factor $\delta_p=(2+\kappa)/3\kappa=\frac{5}{3}$ in the polarization-scrambled fiber compared with the case for only x-polarized light in the polarization-preserving fiber, in which $K=\kappa=1$ leads to $\delta_p=1$. This simplified analysis is valid and is consistent with that based on tensor analysis for these two cases [14]. We note, however, that tensor analysis is required in describing the general case of partial polarization-preserving fibers, which nevertheless is not considered here. Accounting for the enhancement factor and expressing the phase modulation parameter as $u=u_0g$, the coefficient u_0 is then given by

$$u_0=U_0\delta_p\gamma_{ao}/K , \tag{11}$$

where

$$U_0=\frac{4\rho_0 v_a\lambda_P\Delta\nu_B}{\varepsilon_0 n^8 p_{12}^2}n_2 \tag{12}$$

and v_a is the acoustic velocity, ρ_0 the equilibrium density of the medium, p_{12} the longitudinal elasto-optic coefficient, λ_P the wavelength of the pump field, and $n_2=3\chi^{(3)}/8n$ the nonlinear index coefficient. γ_{ao} is the ratio of the optic-optic to the acousto-optic interaction cross sections, which is approximately equal to 1.0 in a single-mode fiber. It is seen from Eqs. (7) and (11) that the factors δ_p and K enhance the effect of phase modulation at the expense of the pump intensity in polarization scrambled fiber. Therefore K, together with δ_p, gives the total enhancement factor

$$\frac{\delta_p}{K}=\frac{2+\kappa}{3\kappa[\kappa^2+(1-\kappa)^2]} , \tag{13}$$

with values of $\frac{10}{3}$ and 1 for the two special cases we consider. It therefore follows that phase modulation is strongest in polarization-scrambled fibers and weakest in polarization-preserving fibers.

We now investigate the boundaries for dynamic instability through numerical linear stability analysis using the pump g and reflectivity $R_1=R_2=R$ as variables. We choose u_0, as the control parameter, to describe the influence of the polarization effects discussed above. The physical parameters chosen, as detailed below, are those for commonly used optical fibers of GeO_2-doped SiO_2 core and a pure SiO_2 cladding pumped at 1.06 μm. Results are shown in Fig. 1, where the curve for $u_0=0$ corresponds to that predicted by Bar-Joseph *et al.* [5]. As can be seen, the instability threshold at low pump intensity is not sensitive to u_0 and is only slightly upward shifted on increasing u_0. At high pump intensity, a large u_0 can, however, lead to a notable extension of the unstable region through an upshift of the upper boundary. For example, the amount of shift of the boundary is $\Delta g\simeq 3.7$ for an increase of u_0 from $u_0=0$ to 0.4. The effect of nonlinear refraction, however, is not only to increase the unstable region, but also to considerably enhance the complexity of dynamic behavior that exists in these regions as described below.

The time-averaged outputs of the transmitted pump and backscattered Stokes signals are shown in Fig. 2 as a function of incident pump signal strength g. As can be seen, the signal strength of the transmitted pump exhibits a plateau, indicative of saturation, while that of the Stokes emission increases almost linearly with the input signal. Here the parameters for polarization-scrambled

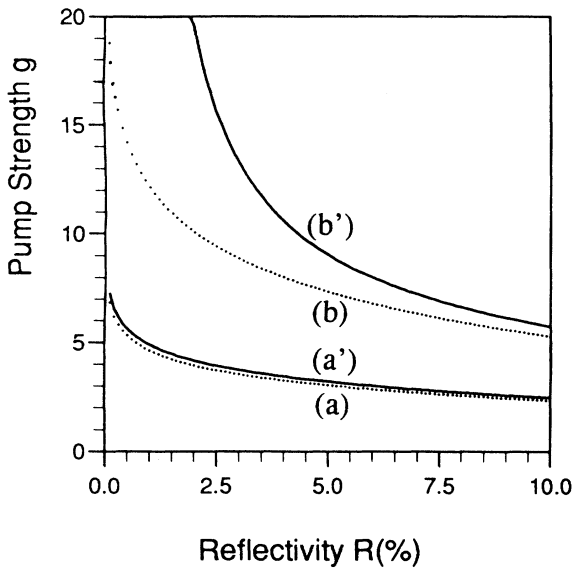

FIG. 1. Instability boundaries in the g-R plane. The dot curves (a) and (b) are calculated using the truncated intensity model by Bar-Joseph *et al.* [5], while the solid lines (a') and (b') are obtained using the full model in Eqs. (1)–(4).

fibers are used for which the enhancement effect gives rise to a value of $u_0=0.4$. A most interesting phenomenon is the pronounced shoulder in the transmitted pump curve where the onset of strong Stokes emission begins. This feature, which is absent in the steady-state solution, is therefore a direct result of the dynamics of SBS. Further, the shoulder effect is found to increase with the value of u_0, implying that increasing the phase modulation slows down the saturation of the pump in this region. The physical constants used in our simulations are those for the silica fiber mentioned above: $\rho_0=2.21\times10^3$ kg/ m^3, $v_a=5960$ m/s, $p_{12}=0.286$, $n=1.4616$, and $n_2=3.85\times10^{-22}$ m^2/V^2 [15]. The spontaneous Brillouin bandwidth for bulk silica is taken as $\Delta\nu_B=33.35$ MHz at $\lambda_P=1.06\mu$m. Due to enhancements in the fiber, this bandwidth can be enlarged by a factor δ_e of 1–2.5 [11,12]. In this analysis we take $\delta_e=2.36$ at $\lambda_P=1.06\mu$m, giving a value for U_0 of 0.12. We note that δ_e is an adjustable parameter in our analysis and its value, which lies well inside the above range, is chosen to give a best fit with our experimental data [1]. We use a fiber length of 124 m corresponding to experiments [1], for which $\beta=0.0414$ for $\alpha=1.45$dB/km at an operating wavelength of 1.06 μm and the corresponding $\beta_A=148$. Using these constants, we have $g_0=4.825\times10^{-11}$ m/V and A_{eff} is calculated to be 27.01 μm^2 for the optical fiber of the core radius $a=2.75$ μm.

The dynamics of the Stokes emissions in the vicinity of and above the threshold for SBS are found to be very distinct in the five regions identified in Fig. 2. In region I, on increasing the pump strength in the vicinity of the threshold $g\simeq3.5$, the Stokes signal emerges from stochastic high-frequency noise to exhibit randomly-amplitude-modulated periodic oscillations at the fundamental period $2T_r$, an example of which is shown in Fig. 3. This random feature is attributable to the effect of aperiodic phase modulation induced by the nonlinear refraction, in the absence of which only limit cycle behavior is obtained. In Fig. 4 we show time series and their corresponding phase portraits obtained in regions II–IV. The boundary between regions I and II, located at $g\simeq5.5$, marks the onset of strong SBS and a transition to stabilized periodic emission (period $2T_r$) in region II [Figs. 4(a) and 4(b)]. The transition to region III at $g\simeq6.4$ marks the emergence of quasiperiodic motion [Figs. 4(c) and 4(d)] with fundamental frequencies $f_1=1/2T_r$ and f_2 being slightly less than f_1, the incommensurability of which is evidenced in the complex features of the power spectra, arising from their various linear combinations. Further bifurcation from this results in aperiodic motion which spans over a parameter window of $6.72<g<9.5$ within region III. A typical time series for $g=7.0$ and the corresponding phase portrait are shown in Fig. 4 [traces (e) and (f)]. Correlation

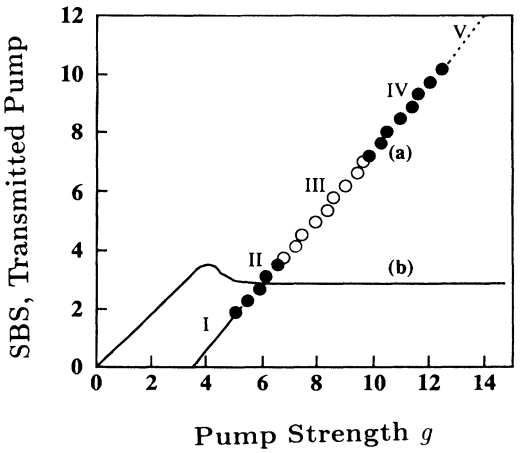

FIG. 2. (a) Time-averaged Stokes signal and (b) transmitted pump intensity as a function of input pump strength g. The regions I–V mark parameter windows of different dynamical behavior.

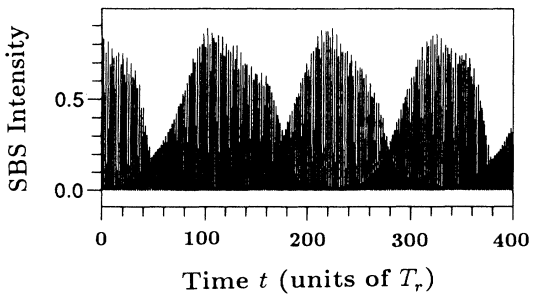

FIG. 3. Time series of the Stokes emission showing random modulation induced by nonlinear refraction for $g=4$ in region I.

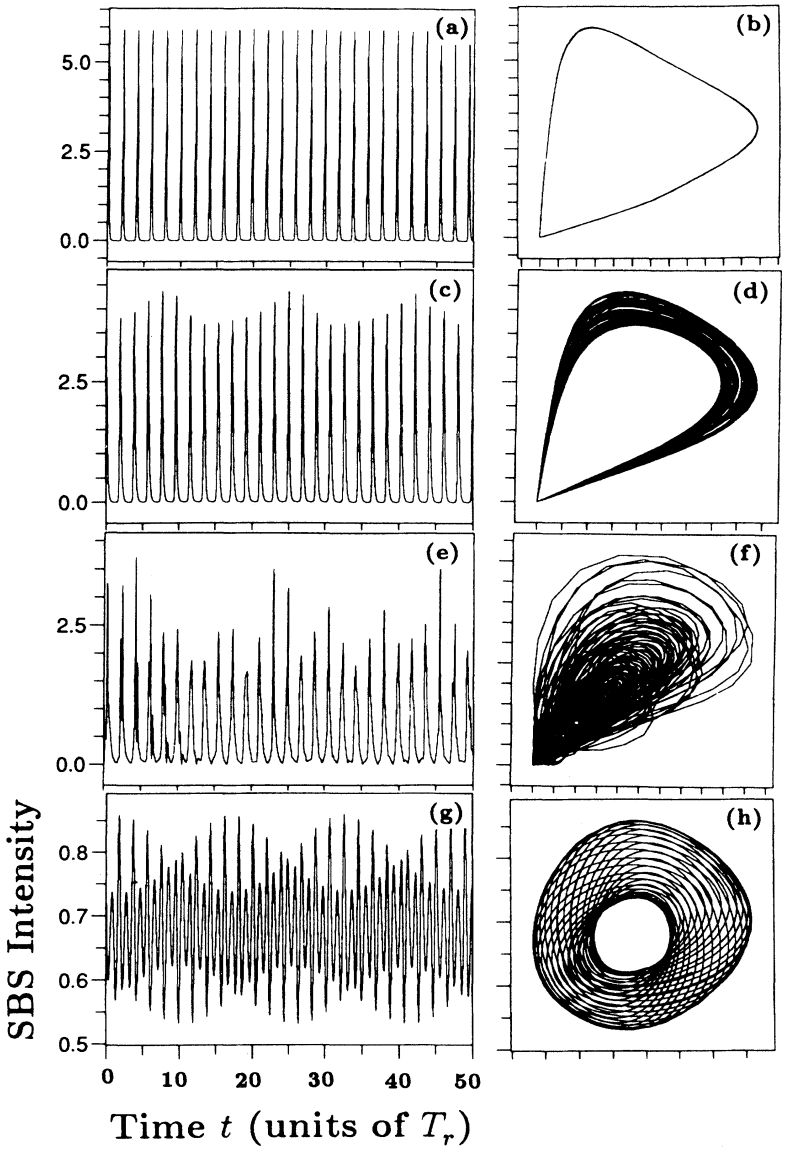

FIG. 4. Time series (left-hand column) and corresponding phase portraits (right-hand column) of the Stokes signals in regions II–IV of Fig. 2. (a) and (b) Periodic motion for $g=5.9$ in region II; (c) and (d) quasiperiodic motion for $g=6.5$ in region III; (e) and (f) chaotic motion for $g=7.0$ in region III; and (g) and (h) quasiperiodic motion for $g=10.0$ in region IV. The abscissa and ordinate in the phase portraits are SBS intensities $I(t_i)$ and $I(t_i+T)$, respectively, in which T is the delay time.

dimensional analysis of this data set using the Grassberger-Procaccia algorithm [16] is shown in Fig. 5 and is seen to give a correlation dimension $D_2 \simeq 2.5$. The collective dynamic features over regions II and III suggest a Ruelle-Takens route to chaos [17]. On further increase of the pump strength an inverse bifurcation sequence takes place, with chaos collapsing through a narrow window of quasiperiodicity [Figs. 4(g) and 4(h)] to steady state. We also find limit cycle behavior in a limited parameter interval within this region. In the region marked IV ranging from $g=9.6$ to 12.3, the quasiperiodicity in general comprises two incommensurate frequencies, one being $1/2T_r$ and the other located close to its higher-order harmonics. The second to fifth orders have been identified in our simulations, each of which depends sensitively on the pump condition. The transition to steady state occurs with a gradual reduction in the ampli-

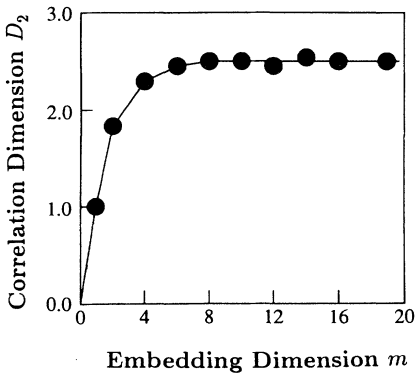

FIG. 5. Correlation dimension D_2 versus embedding dimension m using a data set corresponding to that in Fig. 4(e).

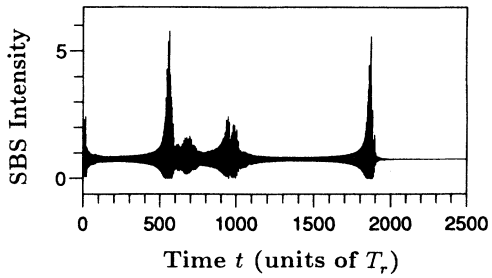

FIG. 6. Stokes signal intensity as a function of time t showing a train of transient random bursts toward the intensity stable state for $g=14.0$ in region V.

tude of the dynamics. The steady-state emission is found to be preceded by a long transient process, with a typical time scale of many thousands of T_r, in some parameter windows exhibiting a train of randomly distributed temporal bursts, a typical example being shown in Fig. 6. It is interesting to note that in region V the Stokes field is periodically modulated even when the intensity output is constant, indicative of the persistence of phase modulation in this process.

Toward establishing the generality of these findings, we have investigated in this theory the dependence of the SBS dynamics on the length L of the fiber, through the parameter β_A, and on the reflectivity R. Numerical simulation shows that there is a critical β_A dependence of the dynamics on the gain g and reflectivity R. Below the critical length, the SBS system is stable. We note that the dynamical behavior is not sensitive to the change of β_A when β_A is well above its critical value. Therefore the fiber length is not critical to the dynamics as long as this condition is satisfied; typically $\beta_A > 10$ ($L > 8$ m) at $g=8$ for the fiber we use. In generating complex temporal structures, lower reflectivities at the two ends are preferred, so a higher pump intensity is required for SBS oscillation, thereby enhancing the effect of phase modulation. In our main analysis we have, however, restricted our consideration to Fresnel reflections so as to interface our results with existing experimental findings.

Our further analysis has established the important dependence of the SBS dynamics on the nonlinear refractive strength u_0. First, in the limit $u_0=0$ corresponding to the conventional model description of SBS [4,5], we find the dynamics to be restricted to periodic oscillation with period $2T_r$ from threshold, which evolves, on increasing the pump parameter, to quasiperiodic motion. The latter motion, confirmed by measuring correlation dimension $D_2=2$, has not been previously reported, though in our analysis we find that it persists over a wide range of parameter values. On further increasing the pump, the quasiperiodicity transfers to steady state at $g \simeq 8.6$. More generally, similar dynamic behavior is found to exist for $u_0 \neq 0$. However, above a critical value $u_0 \simeq 0.3$, aperiodic oscillatory behavior is also found to prevail, evolving via a Ruelle-Takens sequence similar to that described above. We have further investigated the influence of noise initiation of spontaneous Brillouin scattering on the SBS dynamics. We find that from the onset of the SBS oscillation, the noise has no effect on the dynamics of the Stokes emission for both the truncated and our more generalized model descriptions. It follows that (even weak) external feedback is decisive in suppressing the noise which otherwise appears to dominate the emission as evidenced by the stochastic behavior observed in fiber experiments without external feedback [3,7].

Further, we compare our results with earlier experimental findings [2], notably those recently reported on regular and chaotic dynamics [1]. In comparing the time-averaged outputs of the transmitted pump and Stokes emission with those of Ref. [1] we find very good qualitative agreement in regard to their general features and significantly the "shoulder" effect. Quantitative agreement with experimental measurements is also good for both the threshold pump signal and the transmitted time-averaged pump signal in the plateau region. The five regions of dynamical behavior also appear to be in accord with experimental findings for both the transition from randomly modulated oscillations to limit cycle behavior and then the quasiperiodic route to chaos. However, the subsequent quasiperiodicity in region IV as predicted by our theory has not so far been identified in experiments, which show instead only the limit cycle behavior of similar high-frequency contents. While the latter is also predicted by our analysis in this region, its operating window is substantially smaller than that experimentally observed. Beyond this region (in region V), while in theory the Stokes emission tends to stable emission on a time scale of thousands of T_r in some parameter windows exhibiting several transient bursts, in experiment it shows an irregular, sustained train of bursts, the duration of the bursts decreasing and the interval between them increasing with pump strength; an asymptotic tendency toward stable emission, though on a considerably longer time scale. These differences preclude a direct comparison in this region. We note that in other experiments [3] similar sustained bursting has been observed; though, as this was shown to be suppressed by active stabilization of the fiber optic system, the authors attributed this particular feature to environmental noise.

Finally, our theoretical results may help explain the dynamics experimentally observed in polarization-preserving fibers. For such a fiber as used in the experiment in Ref. [3], $K=\kappa=1$. Using $\delta_e=2.36$, we obtain $u_0=0.12$, which is far below the critical value for aperiodic behavior ($u_0 \simeq 0.3$). We find indeed the dynamics in this system to be qualitatively identical to that obtained in the truncated model from the onset of strong SBS emission, showing limit cycle and quasiperiodic behavior for the case of natural reflectivity and only limit cycle behavior for higher reflectivities, e.g., $R_1 R_2 \geq 0.5\%$, the latter of which is consistent with the experimental findings in Ref. [3]. On the other hand, even for the case of $u_0 < 0.3$, differences of temporal behavior for systems with and without nonlinear refraction are obvious in the vicinity of the SBS threshold; limit cycles of $2T_r$ for the case of $u_0=0$ are randomly modulated in the presence of nonlinear refraction ($u_0 \neq 0$), the

depth of which increases with u_0. This provides a further indication of the role of nonlinear refraction even in fibers for which chaotic dynamics is not observable.

In conclusion, we have provided a reasonably complete description of stimulated Brillouin scattering in single-mode optical fibers in the presence of external feedback. The physical model, which accounts for the interplay between the gain, the weak external feedback, and the nonlinear refraction, shows that complex dynamic behavior exists in stimulated Brillouin scattering in polarization-scrambled fibers due to the enhanced nonlinear refractive effect, which includes periodic, quasiperiodic, and chaotic emission as observed in experiments. The theoretical findings can also fairly well explain the various forms of simpler stimulated Brillouin scattering dynamics experimentally observed in polarization-preserving optical fibers.

This work is jointly supported by the United Kingdom Science and Engineering Research Council, the U.S. Air Force Office of Scientific Research, and the EEC Science program.

[1] R. G. Harrison, P. M. Ripley, and Weiping Lu, Phys. Rev. A **49**, 24 (1994).
[2] R. G. Harrison, J. S. Uppal, A. Johnstone, and J. V. Moloney, Phys. Rev. Lett. **65**, 167 (1990).
[3] M. Dämmig, G. Zinner, F. Mitschke, and H. Welling, Phys. Rev. A **48**, 3301 (1993).
[4] A. L. Gaeta and R. W. Boyd, J. Nonlinear Opt. Phys. **1**, 581 (1992).
[5] I. Bar-Joseph, A. A. Friesem, E. Lichtman, and R. G. Waarts, J. Opt. Soc. Am. B **2**, 1606 (1985).
[6] R. W. Boyd and K. Rzążewski, Phys. Rev. A **42**, 5514 (1990).
[7] A. L. Gaeta and R. W. Boyd, Phys. Rev. A **44**, 3025 (1991).
[8] Weiping Lu and R. G. Harrison, Europhys. Lett. **16**, 655 (1991).
[9] Weiping Lu, A. Johnstone, and R. G. Harrison, Phys. Rev. A **46**, 4114 (1992).
[10] See, for example, Y. R. Shen, *The Principles of Nonlinear Optics* (Wiley, New York, 1984).
[11] N. Shibata, R. G. Waarts, and R. P. Braun, Opt. Lett. **12**, 269 (1987).
[12] Y. Azuma, N. Shibata, T. Horriguchi, and M. Tateda, Electron. Lett. **24**, 250 (1988).
[13] G. P. Agrawal, *Nonlinear Fiber Optics* (Academic, Boston, 1989).
[14] B. Crosignani, A. Cutolo, and P. Di Porto, J. Opt. Soc. Am. **72**, 1136 (1982).
[15] J. L. Ayral, J. P. Pocholle, J. Raffy, and M. Papuchon, Opt. Commun. **49**, 405 (1984).
[16] P. Grassberger and I. Procaccia, Phys. Rev. Lett. **50**, 346 (1983).
[17] S. Newhouse, D. Ruelle, and F. Takens, Commun. Math. Phys. **64**, 35 (1978).